

Diffusional transport to and through thin-layer nanoparticle film modified electrodes: capped CdSe nanoparticle modified electrodes

*William G. Hepburn, Christopher Batchelor-McAuley, Kristina Tschulik, Edward O. Barnes,
Roohollah Torabi Kachoosangi⁺, Richard G. Compton**

Department of Chemistry, Physical and Theoretical Chemistry Laboratory, University of Oxford,
South Parks Road, Oxford OX1 3QZ, United Kingdom

⁺now at; C-Tech Innovation Ltd, Capenhurst Technology Park, Chester, CH1 6EH, United
Kingdom

KEYWORDS

Electrochemistry, chemically modified electrodes, quantum dots, cadmium selenide, diffusional
transport, non-electroactive films

ABSTRACT

We present a simple and general theoretical model which accounts fully for the influence of an electrode modifying non-electroactive layer on the voltammetric response of a diffusional redox probe. The layer is solely considered to alter the solubilities and diffusion coefficients of the electroactive species within the thin layer on the electrode surface. On this basis it is demonstrated how, first, the *apparent* electrochemical rate constant can deviate significantly from that measured at an unmodified electrode. Second, depending on the conditions within the layer the modification of the electrode may lead to either *apparent* ‘negative’ or ‘positive’ electrocatalytic effects without the true standard electrochemical rate constant for the electron transfer at the electrode surface being altered. Having presented the theoretical model three experimental cases are investigated, specifically, the reductions of ruthenium (III) hexaamine, oxygen and boric acid on a gold macro electrode with and without a multi-layer organic capped nanoparticle film. In the latter case of the reduction of boric acid the voltammetric reduction is found to be enhanced by the presence of the organic layer. This result is interpreted as being due to an increase in the solubility of the analyte within the non-electroactive layer and not due to an alteration of the standard electrochemical rate constant.

INTRODUCTION

Nanoparticle modified electrodes are a subset of what are more widely termed *chemically modified electrodes*.¹ Historically and presently, the use and development of chemically modified electrodes encompasses a huge amount of research. A thin-film is attached to the electrode surface so as to alter the electrode properties and by design endow it with qualities that are viewed as beneficial. The purpose of the modification is commonly to enable the study of fundamental electrochemical processes^{2, 3} to facilitate the electro-catalysis of a given redox process,⁴ including those important for energy generation,⁵ or for the development of an electrochemical sensor.⁶ In terms of electrochemical sensors the modifying layer often contains redox active moieties (be they organic, biological or nanoparticulate)⁷ that ‘facilitate’ a given electrochemical process and hence enhance the specificity of the sensor. The electrochemical response of such *redox modified* electrodes has been previously approached theoretically.^{8, 9} Conversely, the work presented herein, focusses on the effect of non-electroactive films upon the voltammetry of diffusional redox species. The derived theory is general and applicable to both chemically and nanoparticle modified electrodes.

Non-electroactive organic molecules find common usage as nanoparticle capping agents, serving to protect and stabilize the nanoparticle. The chemical structure of these organics can vary from simple alkyl-thiols to dendritic polymers.¹⁰ Consequently, in the absence of prior capping agent removal¹¹ it is common for an electrode to be co-modified (and electrochemically investigated) with both the material of study and the non-electroactive stabilizing agent present. Beyond the adventitious presence of non-electroactive organics on the electrode surface, a significant number of studies have utilized their presence as a route by which an analyte of interest can be pre-concentrated at the electrode surface.^{6, 12} Of particular importance in this area of study is an early example of polymer modification of a platinum electrode in order to enhance the voltammetric reduction of oxygen.¹³

The work herein presented, develops first a simple model to account for the voltammetry at an electrode modified with a thin-layer of non-electroactive material. Second, experimentally, the voltammetric response of a gold macro electrode with and without modification with organic capped CdSe quantum dots is studied. Electrode modification is achieved through drop-casting a

multi-layer quantity of the nanomaterial onto the electrode surface. From the presented theory it is possible to derive *apparent* electrochemical rate constants, $k_{\text{Red,App}}$ and $k_{\text{Ox,App}}$, for an interfacial redox process. These show how the rate constant for the redox species of interest at the unmodified electrode surface can be *apparently* altered due to the thin layer of modifier. The presence of the modifying film is taken to only alter the solubilities and diffusion coefficients of the electroactive species adjacent to the interface. From a theoretical standpoint the apparent rate constants are evaluated as a function of the applied electrode potential and of major significance is that at high over potentials the rate is shown to be limited by the mass-transport of the electroactive species across the modifying layer. This result for the apparent electrochemical rate constants is generally applicable to the various voltammetric incarnations. As a prime example model cyclic voltammograms are simulated demonstrating the influence of the modifying layer upon electroactive species that exhibit either relatively fast or slow heterogeneous kinetics. Importantly, for redox species exhibiting slow electron transfer kinetics it is predicted that the presence of a thin-modifying layer may - in the case of a higher solubility of the electroactive species in the film (as reflected in the partition ratio) - result in an *apparent* increase in the electron transfer kinetics as evidenced by a shift in the voltammetric peak potential. This theoretical prediction is important as a favorable shift in a voltammetric peak potential is commonly taken to be diagnostic of electrocatalysis; however, the model demonstrates how such a result may solely reflect the altered solubility of the electroactive species adjacent to the electrode.

The influence of the modifying layer on the electrode is experimentally studied using the well-characterised redox probe ruthenium (III) hexaamine. In the presence of the nanoparticulate layer the voltammetry is found to be distorted, with the suppression of the voltammetric peak in a manner which is fully consistent with the mass-transport across the modifying layer being influential on the recorded voltammetry. Having evidenced the applicability of the model for the simulation of the ‘ideal’ voltammetric response of ruthenium hexaamine the final section of the article briefly focuses on two experimentally more complex systems, specifically, the reduction of oxygen and the reduction of the Lewis acid H_3BO_3 . For the irreversible reduction of oxygen it is highlighted how the two-step process of oxygen reduction on the gold electrode is affected differently by the presence of the modifying non-electroactive layer, with the initial reduction process being hindered. Conversely, for the reduction of boric acid the electrochemical process is

found to be *facilitated* by the presence of the non-electroactive modifying layer, giving the illusion of electrocatalysis.

THEORY

This section first presents the derivation of the theoretical model used and highlights the potential dependence of the apparent electrochemical rate constants. This result is general and does not assume anything regarding the applied potential wave form or the prevailing mass-transport regime outside of the modifying layer. Second, simulated examples are provided demonstrating how the altered diffusion regime influences cyclic voltammetric responses for fast and slow electrode processes. The presented theory is applicable to both non-electroactive nanoparticle and chemically modified electrodes.

For a simple one electron redox process the reaction maybe written as;



where A and B are the oxidised and reduced forms of an electroactive species. The presence of a thin modifying layer supported on the electrode will alter the solubilities and diffusion coefficients of the electroactive species adjacent to the electrode surface.

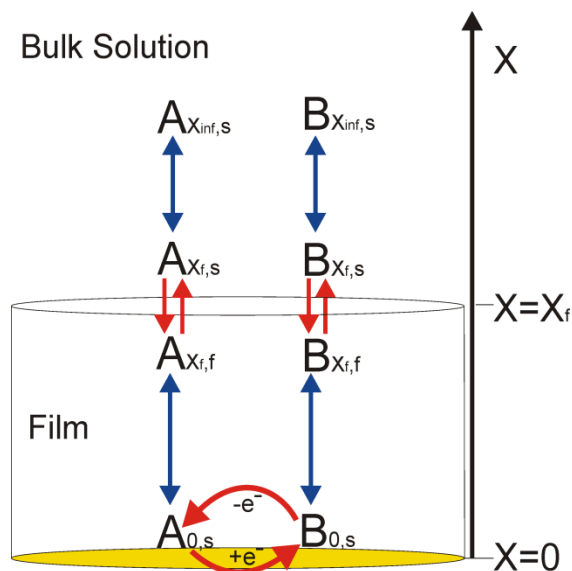


Figure 1. Schematic design of the thin layer model used in this article, where x is the distance perpendicular to the electrode surface ($x=0$). The film thickness is x_f

Figure 1. gives a schematic of the system where x is the distance from the electrode surface (m) and x_f is the film thickness (m). The electroactive species are taken to be able to diffuse freely in and out of the film, where the concentration in each environment is assumed to be at equilibrium such that they may be suitably described by a partition ratio;

$$K_i = \frac{[i]_{x_f,f}}{[i]_{x_f,s}} \quad \text{Equation 2}$$

K_i is the associated equilibrium partition ratio across the film/solution interface (at a distance of x_f from the electrode surface) for the i^{th} species, where $[i]_{x_f,f}$ and $[i]_{x_f,s}$ are the concentrations of the species in the film and the solution respectively. If the thickness of the modifying layer (x_f) is sufficiently small as compared to the diffusion layer thickness ($\delta \sim \sqrt{2Dt}$, where δ is the diffusion layer thickness, D is the diffusion coefficient of the species ($\text{m}^2 \text{s}^{-1}$) and t is the experimental time (s)) then the concentration profiles across the film can be assumed to be approximately linear. From conservation of mass, the flux of material into the film is equal to the flux at the electrode surface.

$$D_{i,f} \left(\frac{\partial [i]_f}{\partial x} \right)_{x=0} = D_{i,s} \left(\frac{\partial [i]_s}{\partial x} \right)_{x_f} = D_{i,f} \left(\frac{\partial [i]_f}{\partial x} \right)_{x_f} = \frac{D_{i,f}}{x_f} ([i]_{x_f,f} - [i]_0) \quad \text{Equation 3}$$

where $D_{i,s}$ and $D_{i,f}$ are the diffusion coefficients of the i^{th} species in the solution and film phase. Recognising that $[i]_{x_f,f}$ can be expressed in terms of K_i and $[i]_{x_f,s}$ and rearranging an expression for the surface concentration can be obtained;

$$[i]_0 = K_i [i]_{x_f,s} - \frac{x_f D_{i,s}}{D_{i,f}} \left(\frac{\partial [i]_s}{\partial x} \right)_{x_f} \quad \text{Equation 4}$$

For the given example of a one-electron transfer, assuming that the electron transfer follows Butler-Volmer kinetics, then the flux at the interface may be described in terms of the diffusion only mass-transport and the electrochemical potential.

$$D_{A,f} \left(\frac{\partial [A]_f}{\partial x} \right)_{x=0} = k_0 [A]_0 e^{-\alpha\theta} - k_0 [B]_0 e^{\beta\theta} \quad \left(\theta = \frac{F(E - E_f^0)}{RT} \right) \quad \text{Equation 5}$$

where k_0 is the standard electrochemical rate constant (m s^{-1}), α and β are transfer coefficients (such that $\alpha + \beta = 1$) and θ is the dimensionless potential. By inputting the appropriate forms of equation 4 into equation 5 and by recognizing that the flux of species B at the interface is equal and opposite to that of species A then, through rearrangement, the flux into the film can be expressed as,

$$D_{A,s} \left(\frac{\partial [A]_s}{\partial x} \right)_{x_f} = \frac{k_0 (K_A [A]_{x_f,s} e^{-\alpha\theta} - K_B [B]_{x_f,s} e^{\beta\theta})}{1 + k_0 x_f \left(\frac{1}{D_{A,f}} e^{-\alpha\theta} + \frac{1}{D_{B,f}} e^{\beta\theta} \right)} \quad \text{Equation 6}$$

The above expression defines the flux at the solution/film interface which is equal to the flux at the electrochemical interface (equation 3). In deriving this equation the effects of migration have been neglected, with the assumption that the system is fully supported outside and inside the film. Moreover, the film and its properties are assumed to be homogeneous across the entire electrode surface. This modified form of the Butler-Volmer equation, as presented in equation 6, fully accounts for the altered kinetics arising due to differing mass-transport regime (within the approximation of a linear concentration profile across the modifying layer). Consequently, equation 6 can be usefully re-expressed in terms of potential dependent *apparent* reductive and oxidative rate constants as defined below;

$$k_{Red,App} = \frac{k_0 K_A e^{-\alpha\theta}}{1 + k_0 x_f \left(\frac{1}{D_{A,f}} e^{-\alpha\theta} + \frac{1}{D_{B,f}} e^{\beta\theta} \right)} \quad \text{Equation 7}$$

$$k_{Ox,App} = \frac{k_0 K_B e^{\beta\theta}}{1 + k_0 x_f \left(\frac{1}{D_{A,f}} e^{-\alpha\theta} + \frac{1}{D_{B,f}} e^{\beta\theta} \right)} \quad \text{Equation 8}$$

where these equations apply at $x = x_f$ and allow the simulation of the solution phase transport without further recourse to any consideration of the diffusion within the film as the effects of this are fully accounted for in equations 7 and 8.

Figure 2 depicts the variation of the $k_{Red,App}$ and $k_{Ox,App}$ as a function of the applied overpotential. Most notably for both the reductive and oxidative rate constants at high overpotentials the electrochemical rate becomes independent of the applied potential. In this high overpotential limit the rate constant simply reduces to;

$$k_{Red,(\theta \ll 0)} = \frac{D_{A,f} K_A}{k_0 x_f} \quad \text{Equation 9}$$

$$k_{Ox,(\theta \gg 0)} = \frac{D_{B,f} K_B}{k_0 x_f} \quad \text{Equation 10}$$

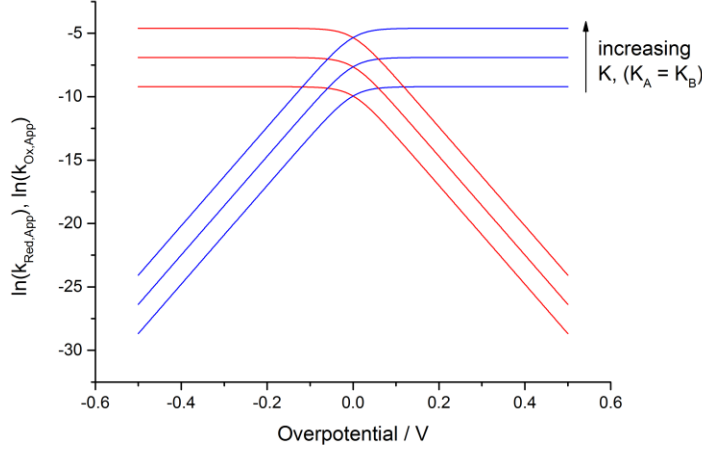


Figure 2: The variation of $k_{Red,App}$ (red line) and $k_{Ox,App}$ (blue line) as a function of the overpotential (V) and the ratio ($K_A = K_B = 0.1, 1, 10$). Other parameters; $k_0 = 0.01 \text{ m s}^{-1}$, $x_f = 100 \text{ nm}$, $D_{A,f} = D_{B,f} = 1 \times 10^{-10} \text{ m}^2 \text{ s}^{-1}$, $\alpha = \beta = 0.5$.

Physically this limit corresponds to the steady-state diffusion across the modifying film being the rate determining process. Conversely, at large underpotentials the potential dependence of the rate constant is greater than that predicted by the Butler-Volmer equation, where for a one electron transfer (with $\alpha + \beta = 1$) the rate is given as below;

$$k_{Red,(\theta \gg 0)} = \frac{D_{B,f} K_A e^{-\theta}}{x_f} \quad \text{Equation 11}$$

$$k_{Ox,(\theta \ll 0)} = \frac{D_{A,f} K_B e^{\theta}}{x_f} \quad \text{Equation 12}$$

Only at low over potentials does the potential dependence of the rate constants k_{Red} and k_{Ox} approximate to that given by the simple Butler-Volmer equation.¹ Specifically, for situations in

¹ These significant deviations from linearity for the log of the apparent electrochemical rate constants versus the applied overpotential in figure 2 highlights why, when using a chemically modified electrode, care must be taken in analysis of the variation of the rate of interfacial electron transfer as a function of potential.^{2,3}

which the ratio of $k_0 x_f / D$ is small and at relatively low overpotentials a third limiting case can be reached in which the numerators in equations 7 and 8 dominate such that the apparent electrochemical rate constants follow a Butler-Volmer type response. To exemplify this point the SI section 1 depicts the variation of the apparent rate constants as a function of film thickness (x_f), with all other variables fixed. A final observation should be made regarding the influence of the partition ratio. As shown in Figure 2), the partition ratio serves to effectively alter the electrochemical rate (note how crossing point for the reductive and oxidative rate constants is shifted as a function of K) via a change in the solubility adjacent to the electrochemical interface without alteration of the standard electrochemical rate constant (k_0).

Using the theory derived above the cyclic voltammetric response of a simple one electron-transfer process (equation 1) at an electrode with a thin modifying layer can be simulated.¹⁴ The results of these simulations are presented in the following section. Further information on the simulation procedure can be found in SI section 2.

THEORETICAL RESULTS

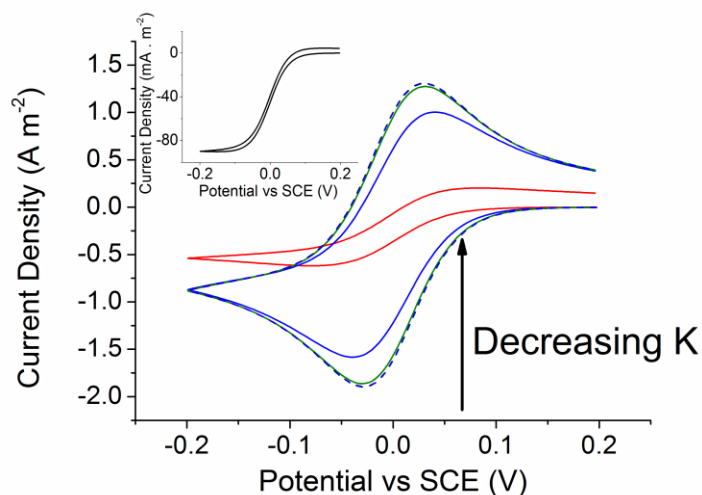


Figure 3: The influence of the partition ratio $K_A = K_B = 0.001$ (black line), 0.01 (red line), 0.1 (blue line) and 1 (green line) [dashed line gives the Nernstian response] on the voltammetry of simple one electron redox couple exhibiting fast electron transfer kinetics $k_0 = 0.01 \text{ m s}^{-1}$. $D_{A,s} = D_{B,s} = D_{A,f} = D_{B,f} = 1 \times 10^{-10} \text{ m}^2 \text{ s}^{-1}$, $E_f = 0 \text{ V}$, $\alpha = \beta = 0.5$, $x_f = 100 \text{ nm}$ and scan rate 500 mVs^{-1} . The inlay depicts the zoomed in plot for $K_A = K_B = 0.001$, showing the steady-state voltammetric response.

Figure 3 depicts the simulated influence of the partition ratio upon the voltammetric response of a simple one-electron redox couple exhibiting fast electron transfer kinetics ($k_0 = 0.01 \text{ m s}^{-1}$). For values of the partition ratio (K) greater or equal to one, the voltammetric response is unaltered from that found for a simple Nernstian process in the absence of a modifying layer. Conversely for values of K below one the voltammetric response is significantly altered, initially resulting in the suppression of the peak current and an increase in the observed peak-to-peak separation. Under conditions where K is significantly below unity the rate of electrochemical reduction reaches near steady-state, where the rate determining process is the mass-transport across the modifying film. An example of this steady-state response is depicted in the inlay of Figure 3 for a value of $K = 0.001$. For K values lying between these two limits ($K = 0.01, 0.1$ for the example in Figure 3) the simulated voltammograms are found to transition between the unperturbed Nernstian semi-infinite diffusional response to that of a steady-state process, as reflected in the decrease in the peak current and the increased peak-to-peak separation. Importantly, over the course of this transition, this *apparent* decrease in the rate of electron transfer (the peak-to-peak separation is found to increase) reflects the dependency of $k_{\text{Red,App}}$ (equation 7) upon the partition ratio K .

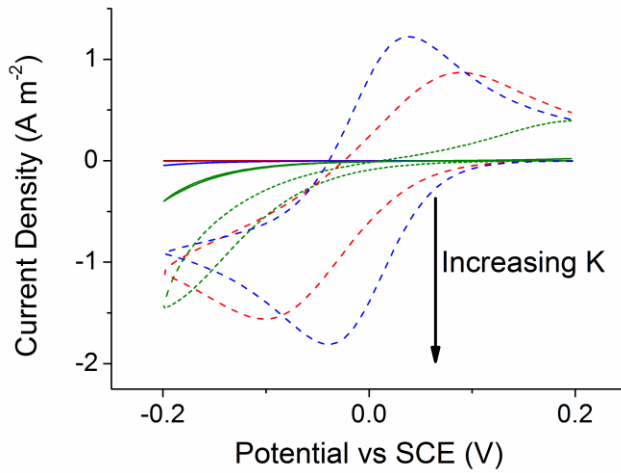


Figure 4: The influence of the partition ratio $K_A = K_B = 0.001$ (black line), 0.01 (red line), 0.1 (blue line), 1 (green line), 10 (green dashed line), 100 (red dashed line), 1000 (blue dashed line) upon the voltammetry of a simple one-electron redox couple exhibiting slow electron transfer kinetics $k_0 = 1 \times 10^{-7} \text{ m s}^{-1}$. $D_{A,s} = D_{B,s} = D_{A,f} = D_{B,f} = 1 \times 10^{-10} \text{ m}^2 \text{ s}^{-1}$, $E_f = 0 \text{ V}$, $\alpha = \beta = 0.5$, $x_f = 100 \text{ nm}$ and scan rate 500 mV s^{-1} .

Figure 4 shows the simulated voltammetric response for a one-electron reduction process exhibiting *slow* electron transfer kinetics ($k_0 = 1 \times 10^{-7} \text{ m s}^{-1}$). For the given simulation parameters the voltammetric response is found to tend towards Nernstian behaviour as the partition ratio, K , increases. This result is of particular note as commonly such a decrease in the voltammetric peak-to-peak separation might be attributed as being due to an “electro-catalytic” effect resulting from an increase in the electrochemical rate constant k_0 . However, in the present example this apparent alteration of the electron transfer kinetics has simply been achieved by the increase in the solubility (increase in K) of the electroactive species adjacent to the electrode, without altering the standard electrochemical rate constant.

The sections below experimentally investigate the reduction of ruthenium (III) hexaamine trichloride ($\text{Ru}(\text{NH}_3)_6^{3+}$), oxygen and boric acid at a gold electrode with a modifying organic layer to validate the above theory.

EXPERIMENTAL

Chemical Reagents

Hexaammineruthenium(III) chloride ($[\text{Ru}(\text{NH}_3)_6]\text{Cl}_3$, Aldrich, 98%), sodium sulphate (Na_2SO_4 , Aldrich, 99%), boric acid (H_3BO_3 , Aldrich, 99.5%) cadmium selenide nanoparticles (CdSe CANdots Series A aqua, CAN GmbH, Hamburg, Germany) and nitrogen (N_2 , BOC, high purity oxygen free) were used without further purification.

Instrumentation

A computer-controlled PGSTAT 20 Autolab potentiostat (Eco-Chemie, Netherlands) was used to operate all the electrochemical experiments. A three electrode set up was used with a saturated calomel reference (BAS Inc. Japan) and a graphite counter electrode. The working electrode was a 1 mm radius gold (Au) macro electrode (CH Instruments Inc.). Before each experiment the working electrode was polished with alumina slurries (0.1, 0.3 and $0.05 \mu\text{m}$) and sonicated in deionised water (30 s) and ethanol (30 s). Subsequently, the electrode was modified with an organic film by casting a droplet of CdSe nanoparticle suspension in water onto the electrode and the solvent was left to evaporate. The nanoparticles have a small CdSe core (diameter 3.5 nm)

with a large organic capping agent (total particle diameter is 28 nm). Further characterization data can be found in the SI section 3.

1.0 mM hexaamineruthenium(III) chloride solutions were made with ultrapure water with resistivity not less than 18.2 MΩ cm at 25°C using 0.1M Na₂SO₄ as the supporting electrolyte and 0.02M H₃BO₃. The solutions were purged for 20 min with N₂ before each experiment and the temperature was controlled at 298±2 K using a thermostatted water bath.

RESULTS AND DISCUSSION

The voltammetric response of an aqueous 1.0 mM ruthenium hexamine solution was studied on a bare gold macroelectrode ($r_0 = 1$ mm) as a function of scan rate (0.01-1.6 Vs⁻¹). Figure 5 depicts the experimentally recorded voltammogram at 0.5 Vs⁻¹, with the inlay depicting the experimentally measured peak current as a function of the square-root of scan rate (the experimental data for the full scan rate range and the invariance of the peak potentials can be found in section 4 of the SI).

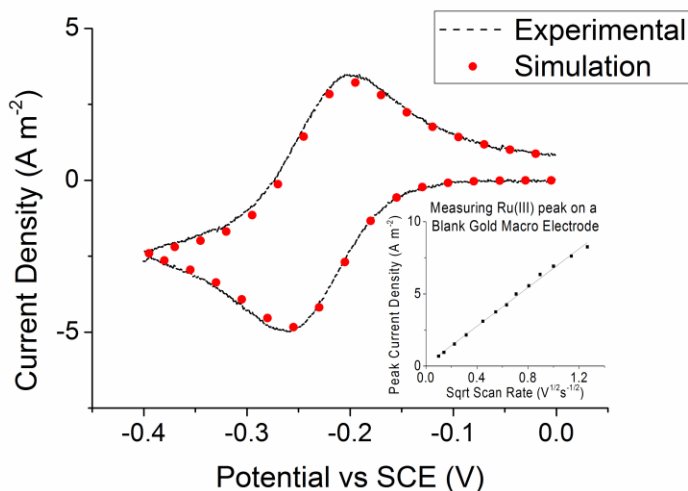


Figure 5: Experimental (black dashed line) and simulated (red circles) voltammetric response of a solution containing 1mM Ru(NH₃)₆³⁺ in 0.1M Na₂SO₄ 0.02M H₃BO₃ on a gold macroelectrode at 500mVs⁻¹. Simulation parameters, $D_{\text{Ru(III)}}=6.2 \times 10^{-10} \text{ m}^2 \text{ s}^{-1}$, $D_{\text{Ru(II)}}=9.6 \times 10^{-10} \text{ m}^2 \text{ s}^{-1}$ $E_f=-0.234$ V vs SCE, $k_0=0.135 \text{ ms}^{-1}$

From the variation of the peak current as a function of scan rate the diffusion coefficient associated with the oxidized species in solution can be measured via the use of the Randles-

Ševčík equation, giving a value of $D_{\text{Ru(III)}} = 6.2 \times 10^{-10} \text{ m}^2\text{s}^{-1}$, which is consistent with previously reported values.¹⁵ Moreover, from the literature the average ratio between the diffusion coefficients for the reduced and oxidized species is found to be 0.65.¹⁵ Using this value and the experimentally determined diffusion coefficient for the oxidized species, it is possible to estimate the diffusion coefficient of the reduced species in solution to be $D_{\text{Ru(II)}} = 9.6 \times 10^{-10} \text{ m}^2\text{s}^{-1}$. The reduction of $\text{Ru}(\text{NH}_3)_6^{3+}$ is thought to proceed via an outer-sphere electron transfer mechanism.¹⁶ Due to the associated large standard electrochemical rate constant for this process on gold, under most experimental conditions the voltammetry at macroelectrodes is found to be fully electrochemically reversible. As a consequence of the experimental challenges associated with measuring such a high electron transfer rate a wide range of values have been reported for the k_0 . However, through the use of a gold nanoelectrode, Mirkin *et al.* have previously measured the standard electrochemical rate constant for the reduction to be $0.135 \pm 0.02 \text{ m s}^{-1}$.¹⁷ This value for the electron transfer kinetics is used throughout the remainder of the article. For the voltammetric response at the bare gold macroelectrode, as presented in Figure 5, the diffusional redox response was simulated using the commercially available software Digisim (version 3.0, BASi Technicol, West Lafayette, IN), the results of which are also depicted.

Having fully quantified the electrochemical reduction of $\text{Ru}(\text{NH}_3)_6^{3+}$ at a bare electrode the influence upon the voltammetry of a thin modifying organic layer was investigated. Polymer capped CdSe nanoparticles were used for the modification, in order to ensure the dots are water stable the CdSe core (diameter = 3.5 nm) is coated with a relatively thick organic layer (12 nm) containing hydroxyl groups to ensure solubility. Modification of the gold electrode surface was achieved through drop-casting 2.6 μl of a 5.0 μM quantum dot stock solution onto the electrode. Assuming a uniform surface coverage this quantity corresponds to the addition of five monolayers of material on to the electrode surface. Figure 6 depicts the recorded voltammetric response at various scan rates, with the inlay showing the measured peak potentials as a function of the logarithm of the scan rate.

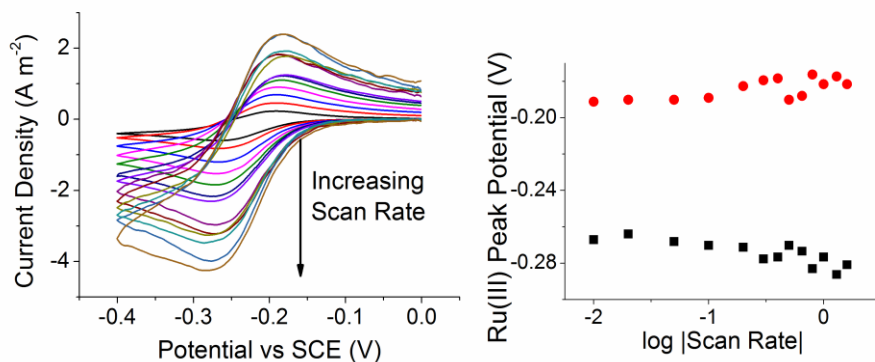


Figure 6: Voltammetry of 1 mM $\text{Ru}(\text{NH}_3)_6\text{Cl}_3$ in 0.1 M Na_2SO_4 0.02 M H_3BO_3 0V to -0.4V on a gold macroelectrode modified with 5 monolayers of organic capped CdSe nanoparticles, scan rates range from 0.01 to 1.6 Vs^{-1} .²

The voltammetric response for the redox process is significantly altered upon modification of the electrode surface with the dropcast organic capped CdSe nanoparticles, where the peak currents are partially suppressed resulting in a voltammogram that appears more sigmoidal in shape. Figure 7 depicts the voltammetry at 0.2Vs^{-1} and experimentally measured peak currents for the $\text{Ru}(\text{NH}_3)_6^{3+}$ reduction as a function of scan rate for various surface coverage of the organic capped CdSe quantum dots. As can be seen for the higher surface coverages and scan rates the measured voltammetric peak is significantly below that obtained on the unmodified electrode. This peak current suppression leads to two significant observations.

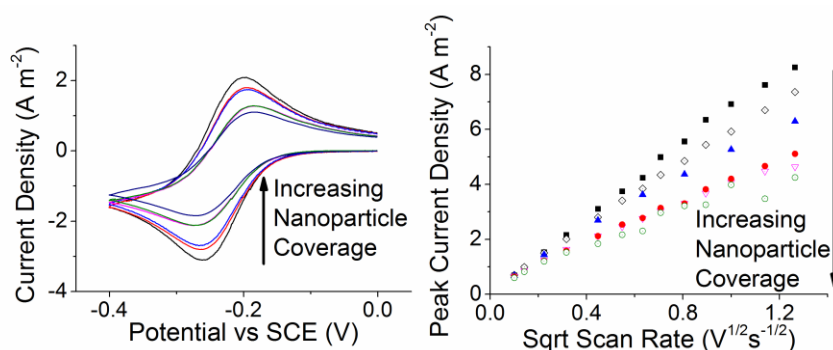


Figure 7: Voltammetry of 1 mM $\text{Ru}(\text{NH}_3)_6\text{Cl}_3$ in 0.1 M Na_2SO_4 0.02 M H_3BO_3 0V to -0.4V scan rate 0.2Vs^{-1} on a gold macroelectrode modified with organic capped CdSe nanoparticles. Experimental peak current as a function of the square root of scan rate for the reduction of $1\text{mM } \text{Ru}(\text{NH}_3)_6^{3+}$, variable surface coverages of organic nanoparticles (corresponding to 0, 0.1, 0.5, 1.5, 3.1 and 5 monolayers).

² The experimental currents have been normalised against the geometric area of the electrode ($3.14 \times 10^{-6} \text{ m}^2$).

First, the plots of peak current versus the square root of scan rate deviates from linearity. Due to the fact that the peak-to-peak separation for the redox couple on the unmodified electrode is found not to increase significantly above the Nernstian value of 60mV, this suppressed peak current cannot be due to systematic uncompensated resistance. Second, for the higher surface coverages the peak current is suppressed to below 79%¹⁸ of the value for the bare electrode. As a consequence of this second observation the decrease in peak height cannot be attributed solely to a decrease in the electron transfer kinetics (k_0). This value of 79% represents the maximum possible change in the peak height (where $\alpha = 0.5$) for the transition from the electrochemically reversible to the electrochemically irreversible limit for a simple one electron transfer at a planar macroelectrode (semi-infinite diffusion).¹⁸ A 50% decrease in voltammetric peak height as measured experimentally would require the alpha value to have a physically unrealistic value of 0.2 (note Mirkin et al. report the transfer coefficient to be 0.45 ± 0.09).¹⁷ Given that the total surface coverage (as defined by area, where 100% represents a monolayer) of the organic capped CdSe nanoparticles is known (504%) and that their diameter is 28 nm, the average film thickness on the electrode surface can be estimated to be 121 nm. Due to the large film thickness it is not feasible for the electron to tunnel across the modifying organic layer, consequently, the electrochemical reduction of the ruthenium hexaamine must be occurring within the organic layer. Hence, it is reasonable to conclude that the suppression of the voltammetric peak height is related at least in part to the mass-transport of the electroactive species across the film.

From consideration of equation 6 within the theory section a number of parameters remain unknown for the modelling of the voltammetric response in the presence of the organic layer. In order to proceed one must reduce the number of variables. Accordingly within this work the following assumptions are made;

$$K = K_A = K_B$$

$$\frac{D_{A,f}}{D_{A,s}} = \frac{D_{B,f}}{D_{B,s}}$$

Using these assumptions and the literature values for the electron transfer kinetics the problem is reduced to the fitting of a two parameter problem, namely K and the ratio D_f/D_s . Using the peak

currents and potentials, as a function of scan rate, as means to assess the accuracy of the fitting, the values of K and D_f/D_s are found to be 0.045 and 0.32 respectively.

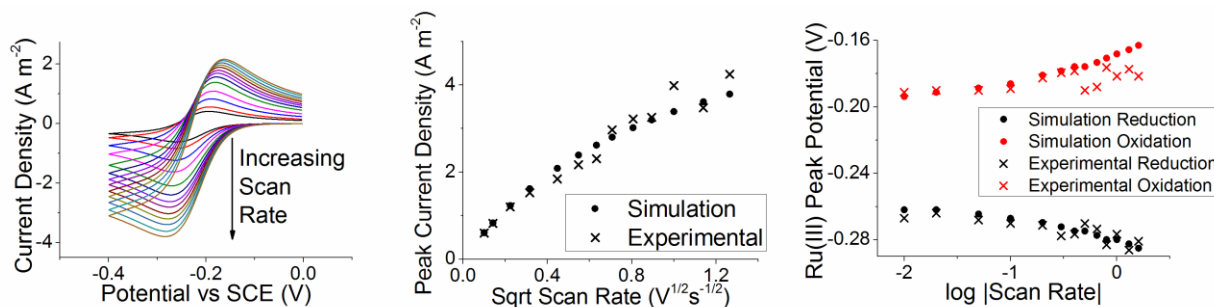


Figure 8: a) Simulated voltammograms at variable scan rates (0.01-1.6 Vs⁻¹) for the reduction of $\text{Ru}(\text{NH}_3)_6^{3+}$ at a gold macroelectrode modified with 5 monolayers of organic capped CdSe nanoprticles. Parameters, $D_{\text{Ru(III),s}} = 6.209 \times 10^{-10} \text{ m}^2 \text{ s}^{-1}$, $D_{\text{Ru(II),s}} = 9.567 \times 10^{-10} \text{ m}^2 \text{ s}^{-1}$, $D_{\text{Ru(III),f}} = 2.0 \times 10^{-10} \text{ m}^2 \text{ s}^{-1}$, $D_{\text{Ru(II),f}} = 3.077 \times 10^{-10} \text{ m}^2 \text{ s}^{-1}$, $E_f = -0.234 \text{ V vs SCE}$, $K_A = K_B = 0.045$, $k_0 = 0.135 \text{ m s}^{-1}$, $x_f = 121 \text{ nm}$, $\alpha = 0.5$, electrode radius = 1mm. B) depicts the variation of the experimental (crosses) and simulated (circles) forward peak currents as a function of the square-root of scan rate. C) depicts the forward (black) and backward (red) peak potentials for the experimental (crosses) and simulated (circles) voltammetric reponses.

Figure 8 a) shows the simulated voltammetric response utilizing the theoretical framework outlined in this article- the data relating to the comparison of the experimental peak currents and peak potentials is depicted in figure 8, b) and c). Importantly, the presented theoretical model is able to fully account for the suppressed voltammetric peak, which is related to the transition towards the mass-transport of the electroactive species across the modifying film being the rate determining process. Having evidenced the validity of the thin-film model for the near-ideal electrochemical redox probe ruthenium hexaamine, we turn to briefly focus upon two more complex examples.

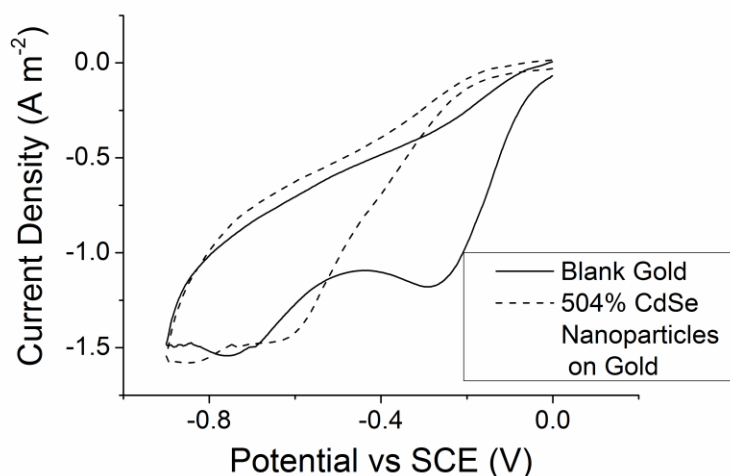


Figure 9: Oxygen reduction on a gold electrode with and without an organic capped nanoparticle film (5 monlayers). 0 V to -0.9 V 50 mVs⁻¹ in 0.1 M Na₂SO₄ 0.02 M H₃BO₃.

The oxygen reduction reaction is of high industrial and academic interest and for the current work provides a good example of an irreversible multi-electron process. Figure 9 depicts the voltammetric response for oxygen reduction on a gold electrode in the presence and absence of a modifying organic layer. At the bare electrode the reduction is found to proceed via two step-wise two-electron transfers, with the corresponding peak currents found at -0.29 and -0.75 V (vs SCE). Upon modification of the electrode the oxygen reduction process appears to be hindered overall as evidenced by the shift in the onset potential for the reduction. Again this shift is suggestive of a partition ratio below unity for oxygen in the modifying film. However, of interest is that the magnitude of the reductive current at ~-0.8V (vs SCE) is not significantly different for the two cases, thus implying that the influence of the organic film is different for the first and second electron transfer processes.

Figure 10 depicts the voltammetric response of a modified and unmodified gold electrode in a solution containing 20 mM H₃BO₃ (0.1 M Na₂SO₄). For the modified electrode an irreversible reductive voltammetric wave is observed at 1.41V (vs SCE). The magnitude of this voltammetric peak is found experimentally to scale linearly with the concentration of boric acid (supporting information section 5). Consequently, due to boric acid being a Lewis acid it is likely that this voltammetric peak in the presence of a modifying organic layer corresponds to proton reduction. Within the literature, previous work has inferred that this apparent enhancement of the reduction

process relates to the mediation of the electron transfer through the CdSe quantum dots.¹⁹

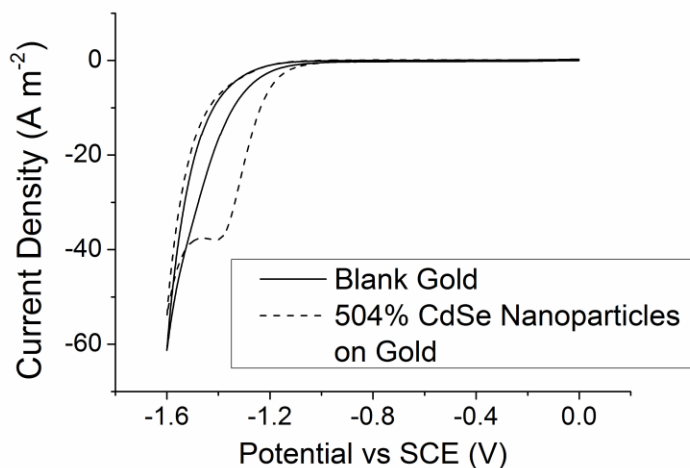


Figure 10: The electrochemical reduction of boric acid on a gold electrode with and without a modifying nanoparticle film. Voltammetric scan between 0 V to -1.6 V (vs SCE) at 50 mV s⁻¹ in 0.1 M Na₂SO₄ and 0.02 M H₃BO₃.

However, in the present experimental example given the thickness of the organic capping layer ('shell') on the individual CdSe cores (12 nm) it is unlikely that the inorganic CdSe core is participating in the electrochemical process. Consequently, in light of the above presented theoretical model the simplest explanation is that the electrochemical reduction is being facilitated by the presence of the non-electroactive organic capping agent within the modifying film. The alteration of the mass-transport adjacent to the electrode leads to the *apparent* electrocatalysis of the reduction.

CONCLUSIONS

A simple and general theoretical model has been developed to account for the influence - upon the voltammetric response of a diffusional redox species - of a thin non-electroactive modifying electrode layer. This layer is only considered to alter the solubilities and diffusion coefficients of the electroactive species. Consequently, the model is applicable to both nano and chemically modified electrodes. The results clearly demonstrate how the rate of the interfacial electrochemical reaction can be significantly altered, such that the apparent rate constants deviate significantly from that predicted by the simple Butler-Volmer equation. Moreover, in the case of a reversible redox species, as experimentally evidenced with ruthenium hexaamine, the rate of electron transfer can be limited by the mass-transport of the electroactive species across the

modifying layer. This hindered diffusion across the organic layer results in this case in a significant suppression of the voltammetric peak height.

Due to the altered mass-transport at the electrode surface the recorded voltammetric response can lead to the electrochemical reaction either being facilitated or hindered depending on the prevailing conditions without a change in the standard electrochemical rate constant (k_0). Beyond the more ideal case of the voltammetry of ruthenium (III) hexaamine, two more complex cases are highlighted. One in which the organic layer hinders the electrochemical process (oxygen reduction) and the other where the rate of reduction appears to be enhanced in the presence of the organic film. This latter example is of particular interest as the enhancement of the reduction process would commonly be interpreted as evidence of electrocatalysis. However, in the framework of the present theory this positive effect can be simply understood in terms of the different solubilities and diffusion coefficients of the electroactive species within the non-electroactive organic layer.

ACKNOWLEDGMENTS

The research leading to these results has received partial funding from the European Research Council under the European Union's Seventh Framework Programme (FP/2007-2013)/ERC Grant Agreement no. [320403]. K.T. was supported by a Marie Curie Intra European Fellowship within the 7th European Community Framework Programme. EOB thanks St. John's College, Oxford for a North Senior Scholarship.

REFERENCES

1. R. A. Durst, A. J. Bäumner, R. W. Murray, R. P. Buck and C. P. Andrieux, *Pure Appl. Chem.*, 1997, 69, 1317-1323.
2. C. Miller, P. Cuendet and M. Grätzel, *J. Phys. Chem.*, 1991, 95, 877-886.
3. C. Miller and M. Grätzel, *J. Phys. Chem.*, 1991, 95, 5225-5233.
4. L. Gorton, *J. Chem. Soc., Faraday Trans.*, 1986, 82, 1245-1258.
5. M. Pumera, Z. Sofer and A. Ambrosi, *J. Mater. Chem. A*, 2014, 2, 8981-8987.
6. R. W. Murray, A. G. Ewing and R. A. Durst, *Anal. Chem.*, 1987, 59, 379 A-390 A.

7. D. W. Kimmel, G. LeBlanc, M. E. Meschievitz and D. E. Cliffel, *Anal. Chem.*, 2011, 84, 685-707.
8. C. P. Andrieux and J. M. Savéant, *J. Electroanal. Chem.*, 1978, 93, 163-168.
9. W. J. Albery and A. R. Mount, *J. Chem. Soc., Faraday Trans.*, 1993, 89, 327-331.
10. Q. M. Kainz and O. Reiser, *Acc. Chem. Res.*, 2014, 47, 667-677.
11. L. M. Fischer, M. Tenje, A. R. Heiskanen, N. Masuda, J. Castillo, A. Bentien, J. Émneus, M. H. Jakobsen and A. Boisen, *Microelec. Eng.*, 2009, 86, 1282-1285.
12. J. F. Price and R. P. Baldwin, *Anal. Chem.*, 1980, 52, 1940-1944.
13. M. R. Van De Mark and L. L. Miller, *J. Am. Chem. Soc.*, 1978, 100, 3223-3225.
14. R. G. Compton, E. Laborda and K. R. Ward, *Understanding Voltammetry: Simulation of Electrode Processes*, World Scientific Publishing Company Incorporated, 2014.
15. Y. Wang, J. G. Limon-Petersen and R. G. Compton, *J. Electroanal. Chem.*, 2011, 652, 13-17.
16. P. Chen and R. L. McCreery, *Anal. Chem.*, 1996, 68, 3958-3965.
17. J. Velmurugan, P. Sun and M. V. Mirkin, *J. Phys. Chem. C*, 2009, 113, 459-464.
18. B. R. Kozub, N. V. Rees and R. G. Compton, *Sensor Actuat. B-Chem.*, 2010, 143, 539-546.
19. A. E. Raevskaya, G. Y. Grodzyuk, A. L. Stroyuk, S. Y. Kuchmiy, E. A. Streltsov, P. V. Chulkin, S. M. Rabchynski and G. A. Ragoisha, 2011.